Energy Proceedings
Vol 45, 2024
ISSN 2004-2965

Primary Frequency Regulation Characteristics Assessment and Allocation of Wind Farm Based on Data-driven Linear MPC

Jiachen Liu[1], Shunqi Zeng[2], Zhongguan Wang[1*], Li Guo[1]

1 School of Electrical and Information Engineering, Tianjin University

2 Guangzhou Power Supply Bureau, Guangdong Power Grid Corporation

ABSTRACT

This paper proposes a data-driven linear model predictive control (MPC) method to assess wind farm capability of primary frequency regulation (PFR) and reasonably allocate droop coefficient to wind turbines (WTs). The proposed method transforms the wind farm PFR nonlinear model into a linear model by using Koopman operator theory (KOT). Hence, a convex optimization problem is constructed based on a linear MPC model, which makes real-time analytical solution possible. Furthermore, the linear model coefficient matrix can be obtained by data-driven training, which is independent of complete model and accurate parameters. The case study validates that the proposed method can achieve high-accuracy assessment and allocation that the relative error is less than 1.60e-2 p.u. by only using historical operation data, and is suitable for online applications owing to the fast calculation speed, which the average assessment time is no more than 0.93s.

Keywords: data-driven, droop control, Koopman, MPC, wind farm.

NONMENCLATURE

Abbreviations	
KOT	Koopman Operator Theory
MPC	Model Predictive Control
PFR	Primary Frequency Regulation
WT	Wind Turbine
Symbols	
$\dot{\omega}_i$	The change rate of *i*-th WT rotor speed
$P_{e,i}$	The active power output of *i*-th WT
J_c	The rotational inertia of the WT
$P_{m,i}$	The mechanical power of the *i*-th WT
ρ	The air density
S	The swept wind area of blade
$v_{w,i}$	The wind speed of the *i*-th WT
$C_{p,i}$	The wind energy utilization coefficient of the i-th WT
$P_{m,i}^0$	The original mechanical power of *i*-th WT before PFR process
$K_{f,i}$	The droop coefficient of *i*-th WT
f_n	The rated frequency
f	The frequency measurement
$\dot{f}$	The change rate of frequency
$K_{f,g}$	The droop coefficient of synchronous generators
K_f	The droop coefficient of the wind farm
ΔP_L	The sudden power mismatch of power system
H	The power system inertia
T	The time step

1. INTRODUCTION

As one of the most widely used renewable energy, wind energy penetration has continuously increased in the last decades [1]. However, WTs interfaces with the grid through power electronic converters, which causes the decoupling of rotor speed and system frequency [2]. Power systems are showing low-inertia feature in many areas. To guarantee frequency stability, WTs are required to participate in PFR.

Variable speed WTs capture kinetic energy from the air, and have a wide speed adjustment range. Hence, the most widely adopted method is adding an extra control module on the power electronic converters, which applies the stored kinetic energy to emulate droop characteristics of traditional generators and regulate frequency [3]. The authors of [4] propose that the WT can regulate frequency by setting the droop gain. In [5] the authors further discuss the regulation of droop gain to avoid excessive use of kinetic which can threaten the operation safety of WTs.

On the wind farm level, the overall droop characteristics should be provided to participate in the

This is a paper for 15th International Conference on Applied Energy (ICAE2023), Dec. 3-7, 2023, Doha, Qatar.

PFR by allocating power among WTs. In [6] power is allocated to WTs in the order of power margin. The authors of [7] propose a centralized MPC method to optimize WT power during PFR process. In our previous work [8] and [9] we propose an energy state index to reasonably allocate PFR power to individual WTs.

In PFR process, it is necessary to maintain rotor speed of all WTs within limit boundary. Therefore, in order to ensure safe operation of WTs, a wind farm should assess the max droop coefficient in different scenarios. The authors of [10] propose that the droop coefficient can be described as a function of WT speed, which adjusts in real-time to prevent the rotor speed from exceeding the limit. Similarly, [11] develops the droop coefficient as a function of WT rotor speed and wind speed. However, three barriers interfere with the application of those physical model-based analysis methods. The first is physical model heavily relies on parameters accuracy and model completeness. With inaccurate parameters, the assessment results definitely deteriorate. The second barrier is the long solution time of large-scale optimization model, which is unsuitable for online application. The last one is the dynamic process of PFR exhibits complex nonlinearity, and hence the solution method isn't off-the-shelf.

With the increasing of installed sensors and calculation capabilities of power systems, researchers exploit the potential of data-driven methods to construct the model in complex conditions. In [12], a double-layer particle swarm algorithm is proposed to optimize power allocation among WTs. A data-driven stochastic projection algorithm is proposed in [13] to optimize wind farm power output. Besides, [14] adopts a data-driven method to assess the healthy operating condition of WTs and adjust their power output, which improves the overall feature of the wind farm.

In [15], the KOT is developed to transform a nonlinear dynamic model into a linear pattern by augmenting the dimension of state space. In our previous work, a linear power flow model is constructed based on the KOT, which shows better accuracy compared to other data-driven methods [16]. The authors of [17] further use the KOT to transform a nonlinear MPC into a linear MPC, which provides a feasible method to solve the nonlinear problem.

This paper develops a data-driven linear MPC method based on KOT to assess the maximum PFR capability of wind farm and achieve the optimal allocation of droop characteristics among WTs.

The remainder of the paper is organized as follows. Section II constructs the physical nonlinear MPC optimization model. The data-driven linear MPC model based on the Koopman operator is developed in Section III and validated by case studies in Section IV. Finally, Section V concludes the paper.

2. PHYSICAL NONLINEAR MPC ASSESSMENT MODEL

2.1 Dynamic Model of Wind Farm

In this section, the dynamic process of wind farm PFR is modeled. For a variable speed WT, the captured mechanical power is

$$P_{m,i}=\frac{1}{2}\rho S v_{w,i}^{3} C_{p,i}\left(\lambda,\beta\right) \tag{1}$$

where $P_{m,i}$ denotes the mechanical power of the *i*-th WT, ρ denotes air density, S denotes the swept wind area of blade, $v_{w,i}$ denotes the wind speed of the *i*-th WT, and $C_{p,i}$ denotes the wind energy utilization coefficient of the *i*-th WT, which can be expressed as a function of the tip speed ratio $\lambda_i = R\omega_i / v_{w,i}$ and the pitch angle β_i, where R denote the paddle radius, and ω_i denotes the rotor speed of *i*-th WT.

The electro-mechanical transient process depends on the unbalance between the mechanical torque $T_{m,i}$ and the electromagnetic torque $T_{e,i}$, which can be expressed as

$$\dot{\omega}_i=\frac{1}{J_{\mathrm{c}}}\cdot(T_{\mathrm{m},i}-T_{\mathrm{e},i})=\frac{1}{J_{\mathrm{c}}}\cdot(\frac{P_{\mathrm{m},i}}{\omega_i}-\frac{P_{\mathrm{e},i}}{\omega_i}) \tag{2}$$

where $\dot{\omega}_i$ denotes the change rate of *i*-th WT rotor speed, $P_{\mathrm{e},i}$ denotes the active power output of *i*-th WT, and J_{c} denotes the rotational inertia of the WT.

A WT can emulate the droop characteristics of synchronous generators by directly regulating its output and responding to system frequency. Hence, the WT output power is related to the frequency change, and can be defined as

$$P_{e,i}=P_{m,i}^{0}+K_{f,i}(f_n-f) \tag{3}$$

where $P_{m,i}^{0}$ denotes the original mechanical power of *i*-th WT before PFR process, $K_{f,i}$ denotes the droop coefficient of *i*-th WT, f_n denotes the rated frequency, and f denotes the frequency measurement.

Since wind farm and synchronous generators provide droop characteristics to regulate frequency, the frequency response is defined as a first-order inertial transfer function:

$$\dot{f}=\frac{f_{\mathrm{n}}}{2H}[(K_{f,g}+K_f)(f_n-f)-\Delta P_L] \tag{4}$$

where $\dot{f}$ denotes the change rate of frequency, $K_{f,g}$ denotes the droop coefficient of synchronous generators, K_f denotes the droop coefficient of the wind farm, i.e., the sum of $K_{f,i}$, ΔP_L denotes sudden power mismatch of power system, and H denotes the power system inertia.

2.2 Nonlinear MPC Assessment Model

To solve the above dynamic model, a general approach is implementing differential discretization to (2) and (4), and the dynamic model can be rewritten as

$$\omega_{i,k+1} = \frac{T \cdot (P_{m,i,k} - P_{e,i,k})}{J_c \cdot \omega_{i,k}} + \omega_{i,k} \tag{5}$$

$$f_{k+1} = f_k + \frac{f_n T}{2H}[(K_{f,g} + K_f)(f_n - f_k) - \Delta P_L] \tag{6}$$

where T denotes time step, and k is the discrete control point.

According to (6), we can transform (3) into

$$P_{e,i,k} = P_{m,i}^0 + K_{f,i}(f_n - f_k) \tag{7}$$

The objective is to assess the maximum K_f of the wind farm and reasonably allocate it to the individual WTs in the entire PFR process, i.e.,

$$\max \quad \sum_{i=1}^{l} K_{f,i} \tag{8}$$

where l denotes the number of WTs.

To ensure the safety of all WTs, the operational constraints of rotor speed are defined as:

$$\omega_{i,\min} \le \omega_{i,k} \le \omega_{i,\max} \tag{9}$$

where $\omega_{i,\max}$ and $\omega_{i,\min}$ are the upper limit and lower limits of WT rotor speed.

Therefore, (5)-(9) are the complete optimization model of wind farm frequency characteristics assessment. However, the mathematical model is a nonlinear programming problem, which is hard to solve analytically. Furthermore, the accuracy of solution is limited by the parameters, and the solution time also inhibits real-time application.

3. DATA-DRIVEN LINEAR MPC ASSESSMENT MODEL

3.1 Koopman-Based Linear Dynamic Model

By observing the state equations in Section II, it can be concluded that the change of rotor speed and frequency mainly depends on the rotor speed and frequency in current state and control variables $K_{f,i}$ and $v_{w,i}$. Hence, the dynamic model can be formulated as

$$[\boldsymbol{\omega}_{k+1}, f_{k+1}] = \delta(\boldsymbol{\omega}_k, f_k, \boldsymbol{u}_k) \tag{10}$$

$$\boldsymbol{u}_k = [\boldsymbol{K}_{f,i,k}, \boldsymbol{v}_{w,i,k}]^T \tag{11}$$

where $\boldsymbol{\omega}_k$ denotes the WT rotor speed vector at k, $\boldsymbol{u}_k \in \mathbb{R}^h$ denotes the control vector composed of droop characteristics and wind speed, $\boldsymbol{K}_{f,i,k}$ denotes the column vector of all $K_{f,i}$ at k, and $\boldsymbol{v}_{w,i,k}$ denotes the column vector of all wind speed at k. Considering the communication and solution delay, $K_{f,i}$ should be a constant in one PFR process.

In order to transform the discrete-time nonlinear model (10) into a linear model to realize analytical solving, we first define $\phi(\boldsymbol{\omega}_k, f_k, \boldsymbol{u}_k)$ as mapping function of state space with augmented observation status:

$$\phi(\boldsymbol{\omega}_k, f_k, \boldsymbol{u}_k) = [\boldsymbol{\omega}_k, f_k, \boldsymbol{\xi}(\boldsymbol{\omega}_k, f_k), \boldsymbol{u}_k]^{\mathrm{T}} = [\mathbf{z}_k, \boldsymbol{u}_k]^T \tag{12}$$

where $\boldsymbol{\xi}(\boldsymbol{\omega}_k, f_k)$ denotes nonlinear mapping function of original state variables at k, and $\mathbf{z}_k \in \mathbb{R}^{N_{lift}}$ denotes the augmented observation state of N_{lift} dimension.

By using N to denote the dimension of mapping function, $\boldsymbol{\xi}(\boldsymbol{\omega}_k, f_k)$ can be expressed as

$$\boldsymbol{\xi}(\boldsymbol{\omega}_k, f_k) = \begin{bmatrix} \xi_1(\boldsymbol{\omega}_k, f_k) \\ \vdots \\ \xi_N(\boldsymbol{\omega}_k, f_k) \end{bmatrix} \tag{13}$$

where $\xi_N(\boldsymbol{\omega}_k, f_k)$ denotes the *N*-th function of $\boldsymbol{\xi}(\boldsymbol{\omega}_k, f_k)$.

The mapping function has multiple typical forms. Owing to its significant nonlinear fitting capability, the 'thin plate spline' radial basis function is selected in this paper:

$$\begin{cases} r_k = \|\boldsymbol{x}_k - \boldsymbol{c}\|_2^2 \\ \xi_i(\boldsymbol{\omega}_k, f_k) = r_k{}^2 \log r_k \end{cases} \tag{14}$$

where $\|\cdot\|_2^2$ denotes the Euclidean norm, r_k denotes the Euclidean distance, $\boldsymbol{x}_k$ denotes the original state variables at k, which is defined as $[\boldsymbol{\omega}_k, f_k]^T$, and $\boldsymbol{c}$ is the basis vector.

According to the KOT [15], (10) can be expressed as a global linear form in augmented state space. Using the mapping function shown in (12), the linear model is defined as:

$$[\boldsymbol{\omega}_{k+1}, f_{k+1}, \boldsymbol{\xi}(\boldsymbol{\omega}_{k+1}, f_{k+1})] = \mathcal{K}\phi(\boldsymbol{\omega}_k, f_k, \boldsymbol{u}_k) \tag{15}$$

where $\mathcal{K}$ denotes the finite-dimensional approximate matrix of the infinite-dimensional Koopman operator, which can be partitioned as

$$\mathcal{K} = [\boldsymbol{A} \ \ \boldsymbol{B}] \tag{16}$$

where $\boldsymbol{A}$ denotes the $N_{lift} \times N_{lift}$ dimensional coefficient matrix corresponding to $\mathbf{z}_k$, and $\boldsymbol{B}$ denotes the $N_{lift} \times h$ dimensional coefficient matrix corresponding to $\boldsymbol{u}_k$.

With (12) and (16), the linear equation (15) is reformatted as linear predictor form [17]:

$$\boldsymbol{z}_{k+1} = \boldsymbol{A} \cdot \boldsymbol{z}_k + \boldsymbol{B} \cdot \boldsymbol{u}_k \tag{17}$$

Since the wind farm historical operation data can be obtained, we define a training set as

$$\begin{cases} \mathcal{X} = \left[z_{k,1}, \ldots, z_{k,L} \right], \mathcal{U} = \left[u_{k,1}, \ldots, u_{k,L} \right] \\ \mathcal{Y} = \left[z_{k+1,1}, \ldots, z_{k+1,L} \right] \end{cases} \tag{18}$$

where $\mathcal{X}$ denotes the input variable data set, $\mathcal{U}$ denotes the control variable data set, $\mathcal{Y}$ denotes the output variable data set, and L denotes the number of samples.

Based on the training set, the matrix $\boldsymbol{A}$ and $\boldsymbol{B}$ can be obtained by solving a least-square problem:

$$\min_{\boldsymbol{A},\boldsymbol{B}} \left\| \mathcal{Y} - \boldsymbol{A} \cdot \mathcal{X} - \boldsymbol{B} \cdot \mathcal{U} \right\|_2^2 \tag{19}$$

The analytical solution to (19) is

$$[\boldsymbol{A}, \boldsymbol{B}] = \boldsymbol{G}^{\dagger} \mathcal{M} \tag{20}$$

where † denotes the pseudoinverse, and $\boldsymbol{G}$ and $\mathcal{M}$ are defined as

$$\boldsymbol{G} = \mathcal{Y} \begin{bmatrix} \mathcal{X} \\ \mathcal{U} \end{bmatrix}^T, \mathcal{M} = \begin{bmatrix} \mathcal{X} \\ \mathcal{U} \end{bmatrix} \begin{bmatrix} \mathcal{X} \\ \mathcal{U} \end{bmatrix}^T \tag{21}$$

3.2 Data-Driven Linear MPC Assessment Model

In the PFR process, WT rotor speed continuously changes. The maximum droop characteristics assessment requests all WTs to make full use of stored kinetic energy and maintain their rotor speed within the range.

Therefore, the objective function of the assessment model remains (8). In the process, the dynamic model of wind farm (17) can be rewritten as a linear MPC model:

$$\begin{bmatrix} \omega_{k+1} \\ f_{k+1} \\ \xi_{k+1} \end{bmatrix} = \boldsymbol{A} \cdot \begin{bmatrix} \omega_k \\ f_k \\ \xi_k \end{bmatrix} + \boldsymbol{B} \cdot \begin{bmatrix} \boldsymbol{K}_f^l \\ \boldsymbol{v}_{\mathrm{w,k}}^l \end{bmatrix} \tag{22}$$

where ξ_k denotes the $\xi(\omega_k, f_k)$ value satisfying the linear recursion relationship.

The assessment model should also satisfy the rotor speed constraint (9). The initial state of wind farm augmented observation can be obtained through measurement and the mapping function, which is given as

$$\boldsymbol{z}_0 = \left[\omega_0, f_0, \xi(\omega_0, f_0) \right] \tag{23}$$

To sum up, (8)-(9), (22)-(23) construct the complete data-driven linear MPC assessment model. Owing to the full linearization, the mathematical model is a convex optimization problem, which guarantees solvability.

3.3 Framework of Assessment and Control

The data-driven linear MPC framework in real wind farm can be divided into two processes: offline training and online assessment and control, which are shown in Fig. 1. and Fig. 2.

1) The offline training process collects WT historical data as the training set to construct the Koopman linear model, and estimate $\boldsymbol{A}$ and $\boldsymbol{B}$.

2) The online assessment and control process use the matrix $\boldsymbol{A}$ and $\boldsymbol{B}$ to construct the linear MPC assessment model and solves it to obtain the maximum droop characteristics of the wind farm. Besides, $K_{f,i}$ is allocated to WTs as a reference of local real-time control. The wind farm maximum droop characteristics K_f can be reported to the dispatch center to realize stability analysis of the whole grid.

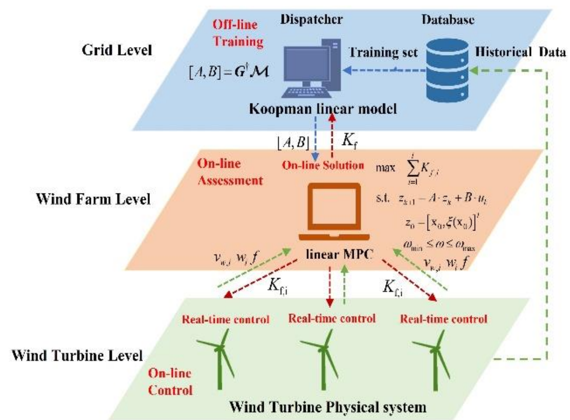

Fig. 1. Data-driven linear MPC assessment framework in real wind farm.

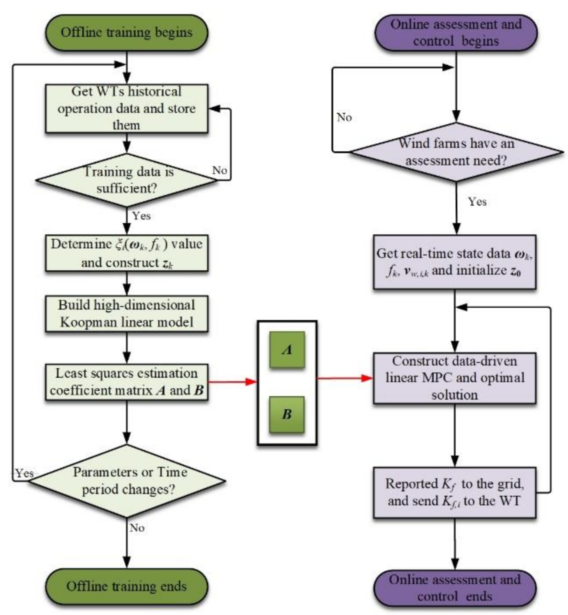

Fig. 2. Data-driven linear MPC assessment process in real wind farm.

4. CASE STUDY

In this section, case studies are carried out in MATLAB to validate the proposed data-driven linear MPC method in frequency different scenarios. The installed capacity of the wind farm is 70 MW, composed of 20 WTs, of which the capacity is 3.5 MW. There are 2 wind measurement towers in the wind farm. The rotor speed limit range is [0.7, 1,3] p.u., and the historical data within [0.73, 1.27] p.u. is used to train linear dynamic model. In this paper, the augmented dimension is 5, dimension of original state variables is 21, and dimension of $\boldsymbol{z}_k$ is 26. The wind speed range is 7-11 m/s. It is assumed that all WTs operate in MPPT mode before participating in PFR. The time step of control point is 0.1 s, and the length of predicted time in MPC is 30 s. We use 12 different wind speed scenarios, which are excluded from the training set, to discuss the linear MPC assessment accuracy, as shown in Fig. 2.

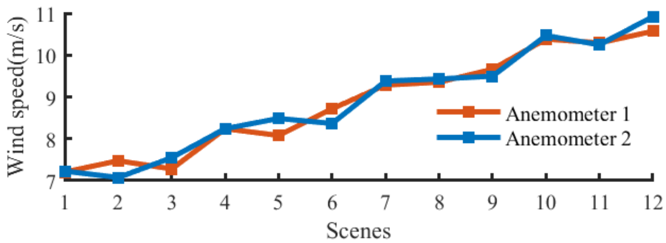

Fig. 2. Wind speed test scenarios.

4.1 Assessment Accuracy

Fig. 3 and Fig. 4 shows the assessment results of K_f and allocation of $K_{f,i}$ in different wind speed scenarios. The assessed optimal coefficients of the model-based MPC based on timing simulation with accurate parameters are considered as the truth value. For comparison, the artificial neural network (ANN), and model-based MPC based on inaccurate parameters, i.e., J_c decreases 5%, H decreases 5%, and R increases 3% from their real value are also carried out. As shown in frequency rising scene, the maximum $K_{f,i}$ shows the opposite trend to wind speed, and the assessment results of linear data-driven MPC are highly approach to truth value compared to ANN and inaccurate model-based MPC. As its counterpart, when frequency dropping, the maximum $K_{f,i}$ shows the same trend to wind speed and the assessment results of linear data-driven MPC are also highly approach to truth value.

The comparison validates that once parameters are inaccurate, physical model methods definitely deviate from the real frequency regulation capability, and the proposed method has the advantage of highly accurate assessment without relying on physical model parameters.

In order to further demonstrate the accuracy of assessment, we compare the data-driven linear MPC method to model-based method with inaccurate parameters and ANN methods. For the inaccurate model-based method, the time-domain simulation and dichotomous method are used to assess K_f.

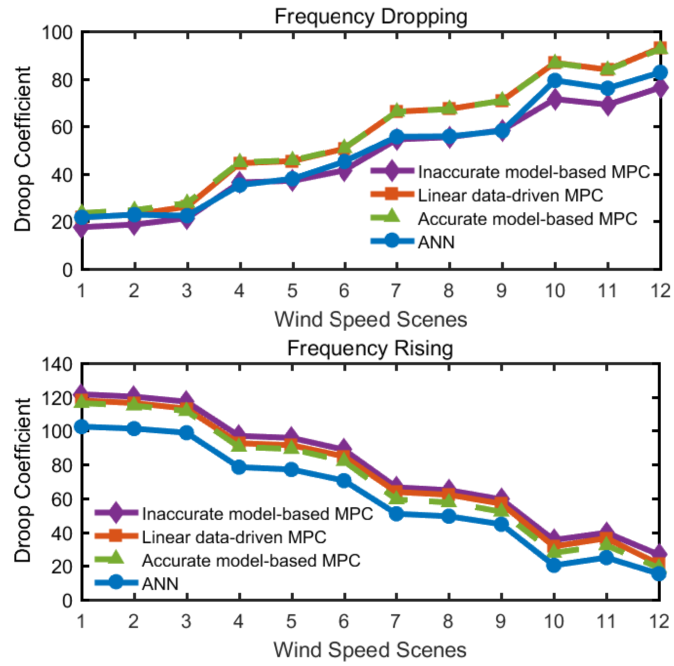

Fig. 3. Assessment results of wind farm droop coefficient in different test scenarios.

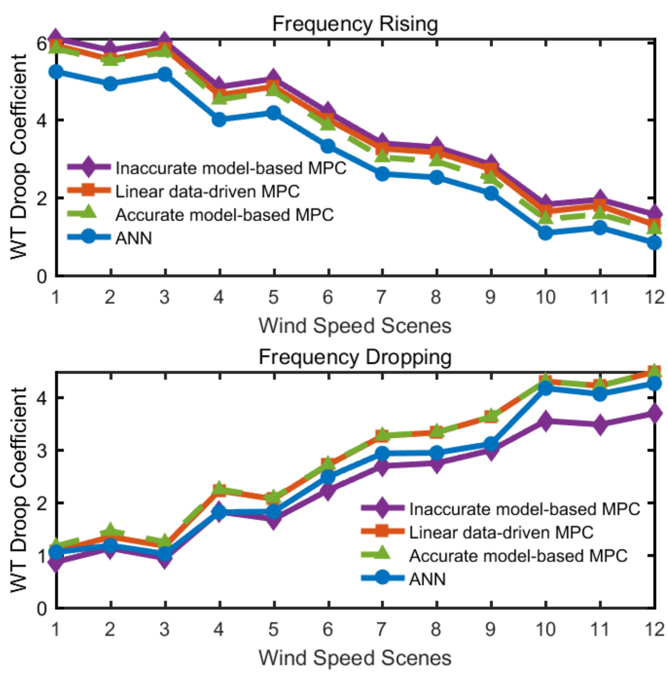

Fig. 4. Assessment results of WT droop coefficient in different test scenarios.

We use the assessed K_f into the accurate nonlinear dynamic model to obtain rotor speed deviation. Table Ⅰ compares the rotor speed root mean square error (RMSE) and maximum absolute error (MAE) in all scenarios. Obviously, the RMSE and MAE values under the proposed method are significantly lower than the model-based method, which demonstrates the accuracy of the proposed data-driven method, and it is also independent of inaccurate parameters impact.

Tab. 1 Comparison of Rotor Speed

Frequency	Method	RMSE (p.u.)	MAE (p.u.)
Rising	Linear data-driven MPC	1.03e-2	1.60e-2
	ANN	3.38e-2	4.30e-2
	Inaccurate model-based MPC	2.17e-2	3.03e-2
Dropping	Linear data-driven MPC	6.91e-3	1.52e-2
	ANN	5.39e-2	5.86e-1
	Inaccurate model-based MPC	1.07e-1	1.91e-1

Furthermore, we discuss the global assessment accuracy by comparing the proposed method and simulation results under accurate model. As shown in Fig. 5 and Fig. 6, the highlight component denotes the scenarios with two wind speed, the difference of which is within 1 m/s. Considering real conditions, these scenarios are more representative. From the results, it can be concluded that the assessment value (left figures) is highly close to the results by simulation test (right figures), which validates the global assessment accuracy. In fact, even in extreme wind speed scenarios, the proposed method still exhibits satisfactory performance.

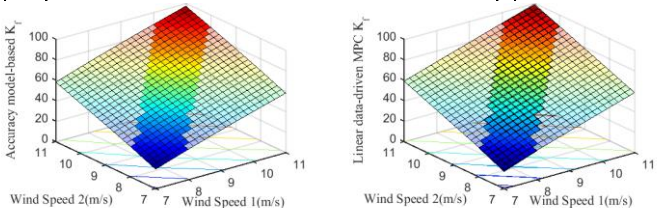

Fig. 5. Comparison of global assessment results of wind farm in frequency dropping scenarios.

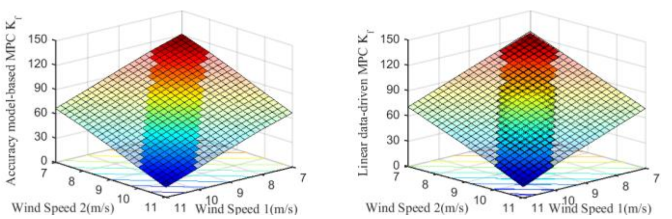

Fig. 6. Comparison of global assessment results of wind farm in frequency rising scenarios.

4.2 Performance of Primary Frequency Regulation

The influence of assessment result to the PFR process is further verified. We both input the assessed results of data-driven and inaccurate model-based methods to dynamic simulation model, and the dynamic variation of rotor speed, wind farm power and WT power are shown in Fig. 6.

As shown in Fig. 6, the proposed method can ensure the rotor speed within the safe range in the whole PFR process. Meanwhile, it makes full use of stored energy of WTs and provides the maximum regulation coefficient.

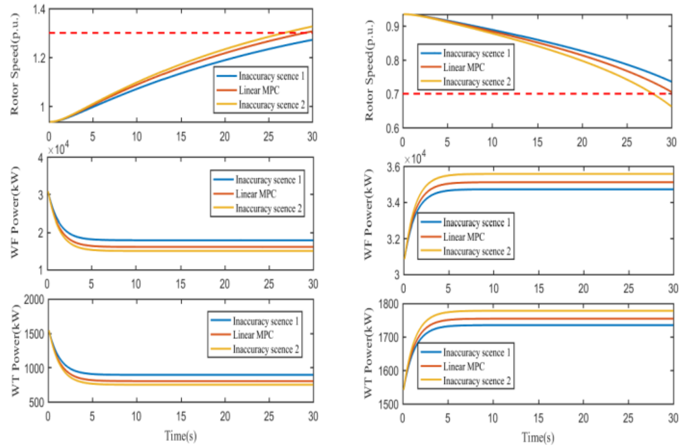

Fig. 7. Comparison of dynamic performance: (a) frequency rising; (b) frequency dropping.

4.3 Calculation Time of Assessment and Allocation

Tab. 2 Comparison Of Calculation Time

Frequency	Average calculation time (s)
Rising	0.93
Dropping	0.89

The calculation time of assessment and allocation is shown in Table II. As shown by the results, owing to the data-driven linear model, the proposed assessment calculation can be finished in one second, which satisfies real-time application requirement.

5. CONCLUSION

This paper develops a data-driven linear MPC model to assess the maximum capability of wind farm PFR, and optimally allocates droop coefficients to each WT. Based on the KOT, the nonlinear MPC model are transformed into the linear MPC form, and hence a convex optimization problem is constructed, which can ensure the solvability. The linear MPC parameters are obtained by data-driven training, and are independent of the static parameters accuracy and model completeness.

The simulation results show that the proposed method has significant accuracy advantages over model-based method under inaccurate parameters. Owing to the data-driven linear model, the solution time is very short, which ensures the proposed method suitable for real-time application.

ACKNOWLEDGEMENT

This work was supported by the National Natural Science Foundation of China under Grant 52007129. (Corresponding author: Zhongguan Wang).

REFERENCE

[1] A. Mitra and D. Chatterjee, "Active power control of DFIG-based wind farm for improvement of transient stability of power systems," IEEE Trans. Power Syst., vol. 31, no. 1, pp. 82-93, 2016.

[2] Z. Zhang, Y. Sun, J. Lin, and G. Li, "Coordinated frequency regulation by doubly fed induction generator-based wind power plants," IET Renew. Power Gener., vol. 6, no. 1, pp. 38, 2012.

[3] P. K. Keung, P. Li, H. Banakar, and B. T. Ooi, "Kinetic energy of wind-turbine generators for system PFR," IEEE Trans. Power Syst., vol. 24, no. 1, pp. 279-287, 2009.

[4] J. Morren, S. W. De Haan, W. L. Kling, and J. Ferreira, "Wind turbines emulating inertia and supporting primary frequency control," IEEE Trans. Power Syst., vol. 21, no. 1, pp. 433-434, 2006.

[5] M. Kayikçi and J. V. Milanovic, "Dynamic contribution of DFIG-based wind plants to system frequency disturbances," IEEE Trans. Power Syst., vol. 24, no. 2, pp. 859-867, 2009.

[6] Awedni, A. Masmoudi, and L. Krichen, "Power control of DFIG-based wind farm for system PFR," in Proc. 15th Int. Multi-Conf. Syst. Signals Devices, Yasmine Hammamet, TUN, 2018, pp. 1298–1304.

[7] Ramtharan G, Ekanayake J B, Jenkins N, "PFR from doubly fed induction generator wind turbines", IET Renew. Power Gener., vol. 1, no. 1, pp. 3-9, 2007.

[8] Z. Wang and W. Wu, "Coordinated control method for DFIG-based wind farm to provide primary frequency regulation service," IEEE Trans. Power Syst., vol. 33, no. 3, pp. 2644-2659, 2018.

[9] L. Guo, Y. Ren, Z. Wang, X. Zhu, X. Wang, X. Li, et al., "Double-layer feedback control method for synchronized frequency regulation of PMSG-based wind farm," IEEE Trans. Sustain. Energy, vol. 12, no. 4, pp. 2423-2435, 2021.

[10] Y. K. Wu, W. H. Yang, Y. L. Hu, and P. Q. Dzung, "Frequency regulation at a wind farm using time-varying inertia and droop controls," IEEE Trans. Ind. Appl., vol. 55, no. 1, pp. 213-224, 2019.

[11] H. Ye, W. Pei, and Z. Qi, "Analytical modeling of inertial and droop responses from a wind farm for short-term frequency regulation in power systems," IEEE Trans. Power Syst., vol. 31, no. 5, pp. 3414-3423, 2015.

[12] Q. Guo, C. Huang, Z. Xue, L. Zhang, X. Lu, and S. Zhang, "Mult-Objective optimization of wind farm dispatch problem by double-layer particle swarm optimization algorithm," in Proc. IEEE 8th Data Driven Control Learn. Syst. Conf., Dali, China, 2019, pp. 728–733.

[13] Z. Xu, H. Geng, and B. Chu, "A hierarchical data-driven wind farm power optimization approach using stochastic projected simplex method," IEEE Trans. Smart Grid, vol. 12, no. 4, pp. 3560-3569, 2021.

[14] M. Schlechtingen, I. F. Santos, and S. Achiche, "Using data-mining approaches for wind turbine power curve monitoring: a comparative study," IEEE Trans. Sustain. Energy, vol. 4, no. 3, pp. 671-679, 2013.

[15] B.O. Koopman, "Hamiltonian systems and transformation in Hilbert space," PNAS, vol. 17, no. 5, p. 315, 1931.

[16] L. Guo, Y. Zhang, X. Li, Z. Wang, Y. Liu, L. Bai, et al., "Data-driven power flow calculation method: a lifting dimension linear regression approach," IEEE Trans. Power Syst., vol. 37, no. 3, pp. 1798-1808, 2022.

[17] M. Korda and I. Mezic, "Linear predictors for nonlinear dynamical systems: Koopman operator meets model predictive control," Automatica, vol. 93, pp. 149-160, 2018.